

## **Stress Analysis and Optimization of Plunger Pump Critical Components**

Wasihun Wondimu Negere

Department of Mechanical Engineering, Institute of Technology, Hawassa University,  
Hawassa, Ethiopia

Corresponding Author's Email: [wasihun962@gmail.com](mailto:wasihun962@gmail.com)

### **ABSTRACT**

This paper presents mechanical strength analysis and optimization of the critical components of the plunger pump. Due to the uneven stress distribution and high contact pressure created between the contacting surfaces the v-packing seals and the PTFE cup were subjected to failure. During the analysis of stresses, the critical components that are considered as a tri-layer compound cylinder such as the assembly of suction tube, PTFE cup, and the check seat and the assembly of plunger, v-packing seals and the spacer tube were analyzed based on the lame's equation of compound cylinders. The materials that are used for making these components were 316 stainless steel and polytetrafluoroethylene or Teflon that are ductile in nature. The failure criteria's which are adopted in this analysis was the maximum shear stress /Tresca criteria and the von-misses criteria's. To optimize the stress distribution in the compound cylinders a classical Lagrangian multiplier method was adopted based on the maximum shear stress theory. The analytically calculated result was compared with the finite element ANSYS simulation software and results from the optimization technique shows that the uneven stress distributions were optimized.

**Keywords:** plunger pump, thick-walled cylinder, tri-layer compound cylinder, stress analysis, Lagrangian multiplier optimization.

### **1. Introduction**

Pumps are mechanical devices used to move fluids from one place to another by converting mechanical energy into hydraulic energy. The prime movers of a pump are: an electric motor, engines, manual power, and etc. Pumps can be classified into two main broad categories, those are: positive displacement pumps and non-positive displacement pumps. Positive displacement pump causes a fluid to move by trapping a fixed amount of it then forcing or displacing that trapped volume into the discharge pipe or a positive displacement pump has an expanding cavity on the suction side and a decreasing cavity on the discharge side. Liquid flows into the pump as the cavity on the suction side expands and the liquid flows out of the discharge as the

cavity collapses. Positive displacement pumps can be classified into rotary positive displacement pumps and reciprocating positive displacement pumps. In the suction stroke the plunger is pulled back, the suction valve opens and the cylinder fills. In the discharge cycle, the plunger moves back, the suction valve closes and the discharge valve opens to deliver fluid. Reciprocating pumps are used for dosing purposes because they are used to move a precise amount of fluid in a specified time period providing an accurate flow rate. Because the head-flow is too shallow peristaltic pumps and centrifugal pumps cannot be used for dosing applications since a small change in differential head/pressure produces a change in the fluid flow (Richard, 2006).

The bottom end of the plunger pump which contains the essential components of the pump is susceptible to failure. Main components of the bottom end of the pump are: suction tube, PTFE cup and check seat. Among the different kind of failures encountered on the bottom end of the plunger pump, failure of the PTFE cup is the major one. Polytetrafluoroethylene (PTFE) is widely used as wear resistant material because it has excellent low friction coefficient when it slides against a metal surface but, the wear rate of PTFE is unacceptably high without filling modification. The sub-assemblies of the bottom end of the plunger pump may be considered as tri-layer compound cylinders. The other stress which has an effect on the compound cylinder is the contact pressure. Contact pressure is created between two cylinders in surface to surface contact. Wear of material during sliding occurs due to the high contact pressure created between the two contacting surfaces.

Plunger pumps used for dosing paints to the fabrics at the Bahir Dar textile factory, which is located in Bahirdar city, Ethiopia are subjected to failure because of the v-packing seals and PTFE cup. Such a failure of the critical components leads to loss of efficiency of the pump and downtime in the industrial machines. Therefore, this study is to analyze and optimize the assembly of check seat, PTFE cup and suction tube assembly.

## **2. Literature Review**

### **2.1. Failures of plunger pump components.**

Under maximum pressure plunger seals fail and their service life decreases. Sealing rings are failed due to stress concentration, contact pressure and the uneven distribution of stresses. And the root reason for the failure of the sealing rings is the inadequate sealing ring structure design (Zhou et al., 2014). The influence of friction created between the seal and the road leads to leakage of a hydraulic system. Once the leakage exceeds the predefined value, the seals are

regarded as failure (Xin Li et al., 2015). Sealing performance and lifetime are depended greatly on the contact pressure and its distribution of the lip. Magnitude of interference is the only way to create contact pressure. Too much interference will result in immoderate drawing and serious wear on the seal lip, while too less will result in leakage (Priit and Andersson, 1999; Zibo et al., 2010; Kaufmann, 2018).

## 2.2. Shrink-fitted compound cylinders

During the shrink fitting of one cylinder over the other a contact pressure will be developed between each layer of the cylinder (Yuan, 2010; Vincenzo, 2014). The value of interference between the shrink fitted cylinders must have to be optimum. When the interference is maximum there will be a higher contact pressure developed between the cylinders leading to wear of the material (Priit and Andersson, 1999). Designing a shrink fit assembly is tricky because the stress developed in the cylinders is a function of internal fluid pressure, shrinkage pressure and the dimensions of the cylinders. Also the shrinkage pressure is a function of the amount of interference and dimensions of the cylinders. to compute the stresses inside compound cylinders, dimensions of the cylinders must be known (Sunil and Patil, 2005). A tri-layer compound cylinder is made by shrink-fitting three cylinders together.

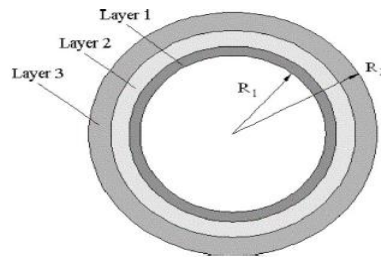


*Figure 2.1: Tri-layer compound cylinder.*

As shown in the above Figure 2.1 the shrinkage/contact pressure is developed between layer 1 and layer 2. And between layer 2 and layer 3 (Hamid, 2005). Inducing the residual compressive stress in these cylinders can improve significantly their capacities such as increasing the working pressure and/or fatigue life. Shrink-fitting techniques are used for increasing the compressive residual stress values and regions in the cylinders wall. The effects of induced tensile stresses due to the working pressure can be decreased by these compressive stresses. (Rahman, 2018) Mojtaba Sharifi (2012) stated that a new analytical solution for the optimum design of shrink-fit multi-layer compound cylinders (Mojtaba and Hematiyan, 2012). This paper presents the optimum design of a multilayer compound cylinder by using analytical optimization technique. Rahman (2018) revealed that maximizing working pressure of autofrettaged three-layer compound cylinders with considering Bauschinger effect and reverse

yielding (Rahman, 2018). This study mainly focused on the effect of interference fit values and autofrettage pressures on three-layer compound cylinders and to design a three-layer compound cylinder by using the combination of shrink-fitting and autofrettage processes to analyze this compound cylinder, Lamé's equation was adopted (Maleki et al., 2010). Residual stress analysis of autofrettaged thick-walled spherical pressure vessel (Farrahi et al., 2010).

This paper studies the residual stress distribution in autofrettage spherical pressure vessels subjected to different autofrettage pressures. Behrooz Farshi et al, (2005), Optimum Autofrettage and Shrink-Fit Combination in Multi-Layer Cylinders (Hamid, 2005). This paper presents a combined shrink fitting and autofrettage of compound cylinders, and the optimum values of the layer thicknesses shrink fitting pressures and autofrettage percentages were determined with the proper sequence of steps. Bahoum et al (2016), Stress analysis of compound cylinders subjected to thermo-mechanical loads (Kaoutar et al., 2016). This research focuses on the resulting stresses and displacement fields in two-layer compound cylinders subjected to internal pressure and logarithmic radial temperature distribution was presented. Ossama and Abdelsalam (2013), Design Optimization of Compound Cylinders Subjected to Autofrettage and Shrink-Fitting Processes (Ossama and Abdelsalam, 2013).

The objective of this study was to identify the optimal configuration of a two-layer compound cylinder subjected to a different combination of autofrettage and shrink fitting and to find out the optimal thickness of each layer, autofrettage pressure, and radial interference. Onur Güngör (2017) an approach for optimization of the wall thickness (weight) of a thick-walled cylinder under axially non-uniform internal service pressure distribution (Onur, 2017). In this study, the mandrel-cylinder tube was renovated by using the constrained optimization method. Wall thickness of the cylinder was optimized to achieve the specified safety factor along the length of the cylinder. Shabana et al. (2017), Stresses minimization in functionally graded cylinders using particle swarm optimization technique (Yasser et al., 2017). In this research work, minimization of the induced stress in functionally graded cylinders due to pressure loading is carried out considering plane stress geometric condition. Majzoobi et al. (2004), Experimental and finite element prediction of bursting pressure in compound cylinders (Majzoobi et al., 2004). This paper presents compound cylinders with different diametric interfaces and various shrinkage radii subjected to bursting and autofrettage pressures.

### **2.3. Optimization techniques for compound cylinders**

In the optimization of the compound cylinders the design variables are the internal and external pressures, thickness of each layer, the autofrettage pressures at the inner surfaces, the autofrettage pressures at the outer surfaces (if any), and the radial interference for shrink-fitting

(Kaoutar et al., 2016). Stresses at each point of cylinders can be calculated using the relations of the stress in thick-walled cylinders in terms of inner and outer pressures of each cylinder. Maximum shear stress and its position can be obtained according to Tresca's yield criterion and using Mohr circle (because the material is ductile). The general formulation for optimum design of compound cylinders using in direct and Lagrangian optimization technique (Mojtaba and Hematiyan, 2012). Compound cylinders can be optimized based on the Simplex procedure of Nelder and Mead, which does not require any gradient evaluation of the life function, treated as the objective. The simplex procedure of optimization technique has good efficiency for a three-layer compound cylinder (Hamid, 2005). generally, from the above literatures it has been inferred that the dosing pump components were not analyzed by assuming the as a compound cylinders. Therefore, this study assumes the assembly of the components as compound cylinders uses the lames equation for the analysis and Lagrangian multiplier method to optimize the dosing pump critical components.

### 3. Materials and methods

The following figure shows the flow chart for the analysis of the plunger pump components (Figure 3.1).

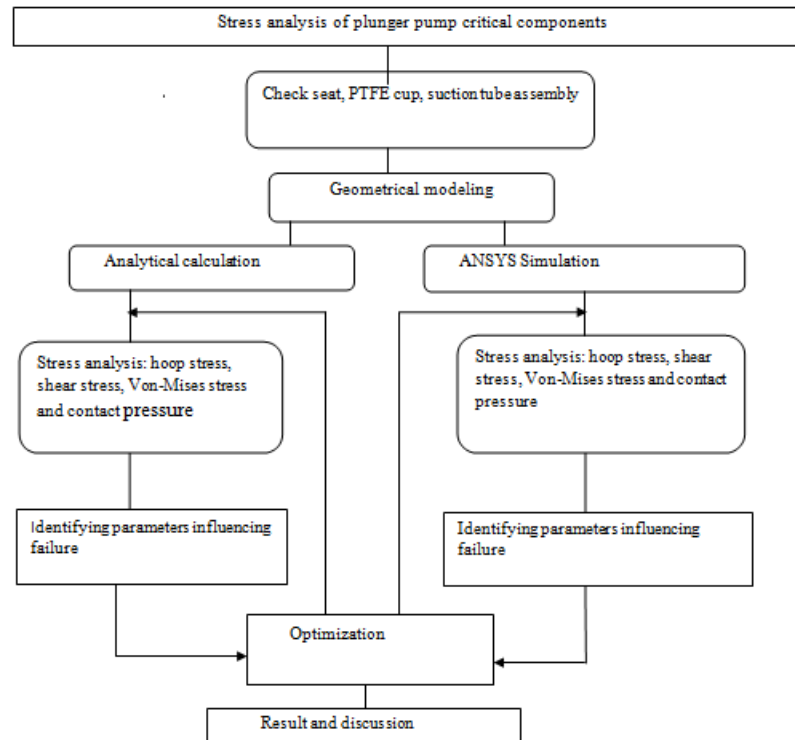


*Figure 3.1: flow chart for the analysis of the plunger pump components*

### 3.1. Materials and geometry

Plunger, check seat and the cylinder in the plunger pump are assembled using the force fitting or shrink fitting techniques. The sub-assembly of the plunger pump containing the cylinder and the plunger as shown in the following figure 3.2 may be treated as a tri-layer compound cylinder formed by shrinking or by force-fit techniques.

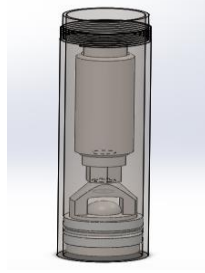


*Figure 3. 2: assemblies of check seat,PTFE cup, and suction tube*

The dimensions were measured using vernier caliper from the dosing pump located at Bahir Dar textile factory and the three-dimensional geometrical modeling were done on solid works. The maximum operating pressure and the mechanical properties of the components are taken from the plunger pump manual located at this particular company. The material used for the cylinder and the plunger is 316 stainless steel and the properties are taken from standard Specification for Chromium and Chromium-Nickel Stainless Steel Plate, Sheet, and Strip for Pressure Vessels and for General Applications ASTM A240/A240M. For the PTFE cup, ASTM D3294-15 is used to characterize the physical properties of polytetrafluoroethylene.

### 3.2. Analysis of check seat, PTFE cup and suction tube assembly by using the Lame's equation

To analyze the stresses, the lames equation can be used. From the lame's theory when the ratio of the thickness to the inside diameter of the cylinder is greater than 1/20, the cylinder is called a thick cylinder. The longitudinal stress is neglected since the cylinder is an open cylinder. In this analysis, the cylinder is considered as thick because the ratio is greater than the above-mentioned number. Thick cylinders can be treated by using the lame's equations as shown below:

$$U_{r,out/r=r_2} = \frac{P_i r_2^3 (1-\nu_1)}{E_1 (r_1^2 - r_2^2)} - \frac{P_i r_1^2 (1+\nu_1)}{E_1 (r_1^2 - r_2^2)} \dots \dots \dots 3.1$$

$$U_{r,in/r=r_2} = \frac{-P_i r_2^3 + P_{ii} r_2 r_3^2 (1-\nu_2)}{E_2 (r_2^2 - r_3^2)} + \frac{(-P_i + P_{ii}) r_2 r_3^2 (1+\nu_2)}{E_2 (r_2^2 - r_3^2)} \dots \dots \dots 3.2$$

$$U_{r,out/r=r3} = \frac{(-P_i r_2^2 r_3 + P_{ii} r_3^3)(1-v_2)}{E_2(r_2^2 - r_3^2)} + \frac{(-P_i + P_{ii}) r_3 r_2^2 (1+v_2)}{E_2(r_2^2 - r_3^2)} \dots\dots\dots 3.3$$

$$U_{r,in/r=r3} = \frac{P_{ii} r_3^3 (1-v_3)}{E_3(r_3^2 - r_4^2)} - \frac{P_{ii} r_3 r_4^2 (1+v_3)}{E_3(r_3^2 - r_4^2)} \dots\dots\dots 3.4$$

For the nested thick-walled cylinders the interference of the inner and outer contact pairs can be determined using the displacement coordination of the corresponding cylinders on the contact surfaces.

$$U_{r,out/r=r2} - U_{r,in/r=r2} = \delta_i \dots\dots\dots 3.5$$

$$U_{r,out/r=r3} - U_{r,in/r=r3} = \delta_{ii} \dots\dots\dots 3.6$$

By substituting the radial displacements in equation 1, 2,3 and 4 into the displacement coordination we can obtain the contact pressure.

Radial and hoop Stress in cylinder 1 (check seat)

From the lame's equation, the hoop stress in cylinder one is given by:

$$\sigma_{\theta} = \frac{P r_4^2 - r_3^2 P_{ii}}{(r_3^2 - r_4^2)} + \frac{r_4^2 r_3^2 (P - P_{ii})}{r^2 (r_3^2 - r_4^2)} \dots\dots\dots 3.7$$

And the radial stress is obtained by the following formula:

$$\sigma_r = \frac{P r_4^2 - r_3^2 P_{ii}}{(r_3^2 - r_4^2)} - \frac{r_4^2 r_3^2 (P - P_{ii})}{r^2 (r_3^2 - r_4^2)} \dots\dots\dots 3.8$$

Where r is any radius in which the hoop and radial stresses can be found

Radial and hoop stress in cylinder 2 (PTFE cup)

In cylinder 2 contact pressure  $P_{ii}$  is acting as an internal pressure and  $P_i$  is acting as an external pressure. Using the lames equation, radial stress in cylinder 2 at inner radius  $r_3$  is given by

$$\sigma_{r3} = -P_{ii} \dots\dots\dots 3.9$$

And the radial stress in cylinder 2 at the outer radius  $r_2$  is ;

$$\sigma_{r2} = -P_i \dots\dots\dots 3.10$$

The hoop stress in cylinder 2 at the outer radius  $r_2$  is given by:

$$\sigma_{\theta ma} = \frac{P_{ii}(r_2^2 + r_3^2)}{(r_2^2 - r_3^2)} - \frac{2P_i r_2^2}{(r_2^2 - r_3^2)} \dots\dots\dots 3.11$$

Hoop stress in the cylinder 2 at the inner radius  $r_3$

$$\sigma_{\theta} = \frac{2P_{ii}r_3^2}{(r_2^2-r_3^2)} - \frac{P_i(r_2^2+r_3^2)}{(r_2^2-r_3^2)} \dots\dots\dots 3.12$$

Radial and hoop stress in cylinder 3(suction tube)

Contact pressure  $P_i$  is acting as internal pressure on cylinder 3 and external pressure  $P_o$  is zero. Therefore the radial stress in the cylinder 3 at the inner radius  $r_2$  is given by:

$$\sigma_r = -P_i \dots\dots\dots 3.13$$

Hoop stress in the cylinder 3 at the inner radius  $r_2$  is given by

$$\sigma_{\theta\max} = \frac{P_i(r_1^2+r_2^2)}{(r_1^2-r_2^2)} \dots\dots\dots 3.14$$

Hoop stress in the cylinder 3 at the inner radius  $r_1$  is given by

$$\sigma_{\theta} = \frac{2P_i r_3^2}{(r_1^2-r_2^2)} \dots\dots\dots 3.15$$

The hoop stress at any radius  $r$  in the compound cylinder due to internal pressure only is given by

$$\sigma_{\theta} = \frac{Pr_4^2}{(r_1^2-r_4^2)} \left[ 1 + \frac{r_4^2}{r^2} \right] \dots\dots\dots 3.16$$

Where  $P$  is the internal pressure and  $r$  is any radius.

Resultant hoop stress in cylinder 1

Maximum hoop stress at the inner surfaces of cylinder 1 at  $r_4$

$$\sigma_{\theta 1} = \frac{P(r_1^2+r_4^2)}{(r_1^2-r_4^2)} - \frac{2P_{ii}r_3^2}{(r_3^2-r_4^2)} \dots\dots\dots 3.17$$

Resultant hoop stress in cylinder 2

$$\sigma_{\theta 2} = \frac{Pr_4^2(r_1^2+r_3^2)}{r_3^2(r_1^2-r_4^2)} + \frac{P_{ii}(r_2^2+r_3^2)-2P_i r_2^2}{(r_2^2-r_3^2)} \dots\dots\dots 3.18$$

Resultant hoop stress in cylinder 3

$$\sigma_{\theta 3} = \frac{Pr_4^2(r_1^2+r_2^2)}{r_2^2(r_1^2-r_4^2)} + \frac{P_i(r_1^2+r_2^2)}{(r_1^2-r_2^2)} \dots\dots\dots 3.19$$

### 3.2. 1.The failure theories

Failure of solid materials under the action of external loads can be predicted using the science of failure theories. Usually, the failure of a material can be classified into brittle failure/ fracture and ductile failure /yield. depending on the varies conditions including the state of stress, temperature, loading rate and etc. in most practical cases a material may fail under brittle or



ductile or both (Khurmi and Gupta, 2005). The failure theories which are mostly used for ductile materials are: Maximum shear stress (MSS) and Distortion energy (DE).

### Tresca criteria:

For thick cylinder design, the Tresca (maximum shear stress) criterion is normally used for ductile materials. The maximum shear stress at the yield in tension is equated to the maximum shear stress in the cylinder wall

$\tau_{max} = \frac{\sigma_y}{2}$ , the maximum shear stress is at the inside radius.

$$\tau_{max} = \frac{\sigma_{\theta} - \sigma_r}{2}, \text{ for cylinder failure } \frac{\sigma_y}{2} = \frac{\sigma_{\theta} - \sigma_r}{2} \dots\dots\dots 3.20$$

Where  $\sigma_{\theta}$ ,  $\sigma_r$  and  $\tau_{max}$  are the maximum hoop stress, radial stress and maximum shear stress respectively.

**Von Mises criteria:** The Von Mises theory (distortion-energy theory) predicts that yielding occurs when the distortion strain energy per unit volume reaches or exceeds the distortion strain energy per unit volume for yield in simple tension or compression of the same material

$$S_y \leq \left[ \frac{(\sigma_{\theta} - \sigma_r)^2 + (\sigma_r - \sigma_l)^2 + (\sigma_l - \sigma_{\theta})^2}{2} \right]^{\frac{1}{2}} \dots\dots\dots 3.21$$

In the Von-Mises criteria yield would occur when  $\sigma \geq S_y$

Table 3.1: Input parameters for the subassembly of plunger and cylinder

| Name of components                             | Cylinder 1<br>(suction tube) | Cylinder 2( ptfе cup)   | Cylinder 3<br>(check seat) |
|--|------------------------------|-------------------------|----------------------------|
| Materials                                      | 316 stainless steel          | polytetrafluoroethylene | 316 stainless steel        |
| Inner radius                                   | 23.25mm                      | 19.7mm                  | 10.35mm                    |
| Outer radius                                   | 26.8mm                       | 23.4mm                  | 19.8mm                     |
| Youngs modulus                                 | 1.93e5Mpa                    | 1.5e3Mpa                | 1.93e5Mpa                  |
| Poissons ratio                                 | 0.31                         | 0.41                    | 0.31                       |
| Tensile yield strength                         | 205 MPa                      | 48.23MPa                | 250 MPa                    |
| Interference between cylinder 1 and cylinder 2 | 0.1mm                        |                         |                            |
| Interference between cylinder 2 and cylinder 3 |                              | 0.15mm                  |                            |
| Maximum operating pressure                     | 4.14Mpa                      |                         |                            |

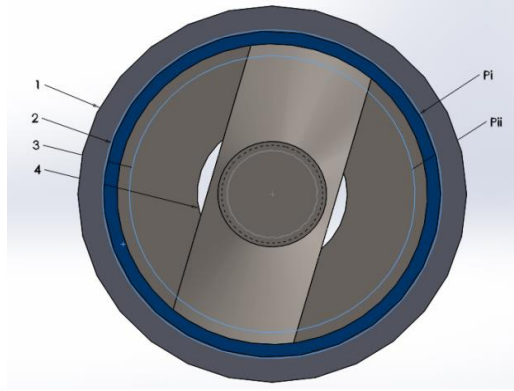


Figure 3.3: Assembly of check seat,PTFE cup, and suction tube.

### 3.2.2. Evaluation of stresses using analytical technique and finite element ANSYS simulation software

Table 3.2: The contact pressure between cylinders in MPa

|          | Analytical | Simulation |
|----------|------------|------------|
| $P_{ii}$ | 7.142      | 7.934      |
| $P_i$    | 9.549      | 10.007     |

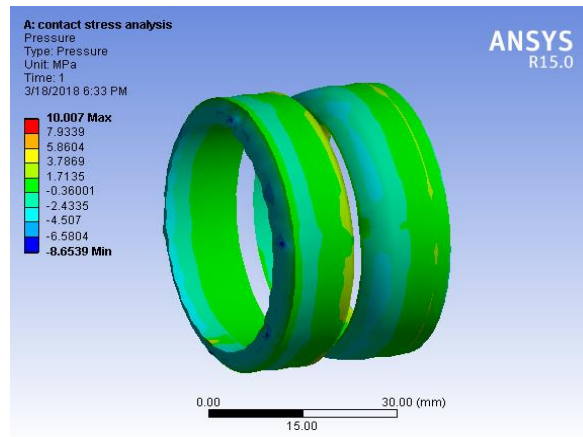


Figure 3.4: Contact pressure distribution

Table 3.3: Maximum hoop stress in MPa

| In Cylinder 1 |        | In Cylinder 2 |        | In Cylinder 3 |        |
|---------------|--------|---------------|--------|---------------|--------|
| classical     | ANSYS  | classical     | ANSYS  | classical     | ANSYS  |
| 72.495        | 81.966 | 22.035        | 23.487 | 14..063       | 11.792 |

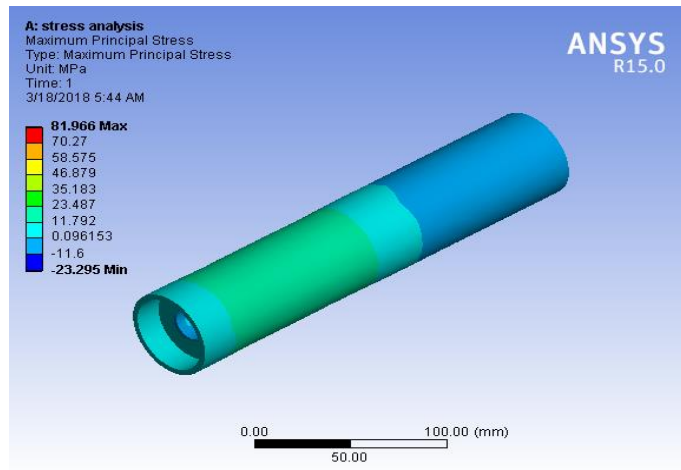


Figure 3.5: Maximum hoop stress

Table 3.4: Maximum shear stress in MPa

| In Cylinder 1 |        | In Cylinder 2 |        | In Cylinder 3 |        |
|---------------|--------|---------------|--------|---------------|--------|
| classical     | ANSYS  | classical     | ANSYS  | classical     | ANSYS  |
| 41.2493MPa    | 40.623 | 12.67MPa      | 14.508 | 10.6MPa       | 11.607 |

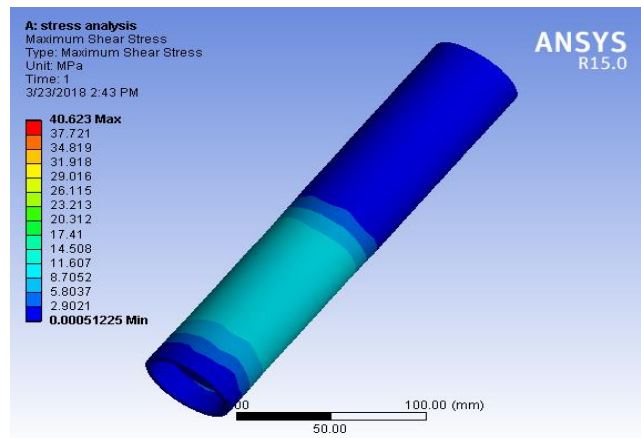


Figure 3.6: Maximum shear stress

Table 3.5: Von Mises stress in MPa

| In Cylinder 1 |       | In Cylinder 2 |       | In Cylinder 3 |       |
|---------------|-------|---------------|-------|---------------|-------|
| classical     | ANSYS | classical     | ANSYS | classical     | ANSYS |
|               |       |               |       |               |       |

|        |       |        |       |        |       |
|--------|-------|--------|-------|--------|-------|
| 78.163 | 73.18 | 28.056 | 32.52 | 18.631 | 16.27 |
|--------|-------|--------|-------|--------|-------|

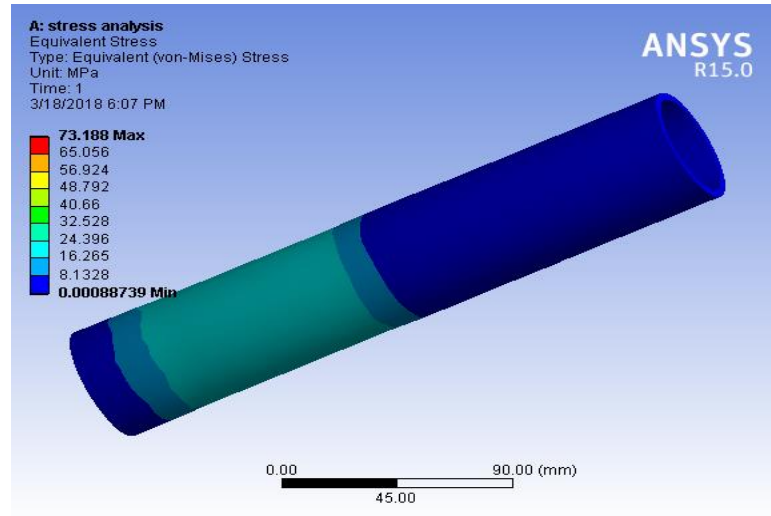


Figure 3.7: Equivalent Von Mises stress

### 3.3. Optimization of the suction tube, PTFE cup, and check seat assembly

During the optimization of a shrink-fitted compound cylinder using the maximum shear stress theory as a design criterion assuming that the inner and outer radii of the multi-layer cylinder and material of each layer are known. The optimization mathematical model was built and Lagrangian multiplier method the model was used to optimize the components. In this analysis, the optimum design formula of the wall ratio “Km” of each layer of the multi-layer cylinder are obtained based on the superposition principle and optimum shrinkage pressure as well as radial interference were also derived and the stress distribution in each layer is analyzed.

Lame’s equation can be written by using the wall ratio K, where K is the ratio of outer of the outermost cylinder to inner radii of the innermost cylinder. Substituting the wall ratio into the principal stress components the hoop and radial stresses will be re-written as follows (Yuan, 2010)

$$\sigma_{\theta} = \frac{(P-P_{ii})k^2}{(k^2-1)} + \frac{r_i^2 k^2 (P-P_{ii})}{r^2 (k^2-1)} \dots\dots\dots 3.22$$

$$\sigma_r = \frac{(P-P_{ii})k^2}{(k^2-1)} - \frac{r_i^2 k^2 (P-P_{ii})}{r^2 (k^2-1)} \dots\dots\dots 3.23$$

Where  $r_i$  is the interference between the two layers and it is given by  $r_i = d_i/2$ , and  $r$  is the arbitrary radius. The maximum shear stress  $\tau_{max}$  is given by

$$\tau_{max} = \frac{\sigma_{\theta} - \sigma_r}{2} = \frac{r_i^2 k^2 (P - P_{ii})}{r^2 (k^2 - 1)} \dots\dots\dots 3.24$$

### 3.3.1. Building the Mathematical Model of Optimum Design

#### 3.3.1.1. Assumptions

It is assumed that the inner and outer diameters of the vessel are known, that the yield stress of each layer is also known, and the assembly sequence in each cylinder is consecutive from inside to the outside of shrink-fitting.

#### 3.3.1.2. Optimum mathematical model

For Ultra-high pressure vessels usually made of the plastic material and alloy steel it is generally thought that failure mode is plastic yield. Therefore, the maximum shear theory for the design criteria. According to the maximum shear theory.

$$\tau_{max} = \frac{\sigma_s}{2} \dots\dots\dots 3.25$$

Eq. (3.24) shows that shear stress changes only in accordance with a pressure difference between the inner wall and an outer wall, and the shear stress has no relation to the absolute value of pressure. When the pressure difference of a vessel is defined, shear stress in the inner wall is maximal, i.e., the dangerous section is in the inner wall of each cylinder. The optimal design of multi-layer vessels requires the maximum use of materials and gives full play to the characteristics of the materials. With the increase of pressure, the shear stress of each layer reaches its shear yield limit, and each layer of cylinder fails at the same time. According to the above requirements and in the utmost limit, the shear stress of the inner wall of layer  $m$  can be written as

$$\tau_{max} = \frac{\sigma_s}{2} = \frac{r_i^2 k^2 (P - P_{ii})}{r^2 (k^2 - 1)} \dots\dots\dots 3.26$$

According to the assumption,  $K$  is a constant, so multi-layer shrinkage vessels have optimization problems as follows

$$\prod_{m=1}^n k_m = k \dots\dots\dots 3.27$$

### 3.3.2. Lagrangian multiplier method

The basic idea of this optimization technique is to turn the equality constraint into non-constraint. This paper uses the Lagrange multiplier method, taking  $\lambda$  as Lagrange multipliers, and  $\sigma_s$  as a constant. During the optimization of a shrink-fitted compound cylinder using the classical Lagrangian multiplier method based on the maximum shear stress theory as a design criterion the following assumptions were taken into account:

- The inner and outer diameters of the vessel are known
- The yield stress of each layer is also known
- Material of each layer were known
- the internal pressure is constant

Optimum geometry for the assembly of suction tube, PTFE cup and check seat in this way, the above-mentioned problems can be transformed into the extremum problems as the following equation:

$$L = \frac{1}{2} \sum_{m=1}^n \alpha_m \frac{(k_m^2 - 1)}{k_m^2} + \lambda (\prod_{m=1}^n k_m = k) \dots \dots \dots 3.28$$

$$\frac{\partial L}{\partial k_m^2} = \alpha_m \frac{1}{k_m^3} + \lambda \frac{K}{k_m^2} = 0$$

$$\frac{\partial L}{\partial \lambda} = \prod_{m=1}^n k_m - k = 0$$

To solve the system of nonlinear, we find the optimal solution of  $km$  as:

$$K_m = \left( \frac{\alpha_1 \alpha_2 \alpha_3 \dots \alpha_N}{\alpha_m} \right)^{\frac{1}{2N}} \alpha_m^{\frac{N-1}{2N}} K^{\frac{1}{N}} \quad m = 1, 2, 3 \dots N \dots \dots 3.29$$

$$k_1 = (\alpha_2 \alpha_3)^{\frac{1}{6}} \alpha_1^{\frac{2}{6}} k^{\frac{1}{3}}$$

$$k_2 = (\alpha_1 \alpha_3)^{\frac{1}{6}} \alpha_2^{\frac{2}{6}} k^{\frac{1}{3}}$$

$$k_3 = (\alpha_1 \alpha_2)^{\frac{1}{6}} \alpha_3^{\frac{2}{6}} k^{\frac{1}{3}}$$

The contact pressure between cylinder 1 and 2 is given by:

$$p_i = \left( P - \frac{\sigma_s k_1^2 - 1}{2 k_1^2} \right) \dots \dots \dots 3.30$$

The contact pressure between cylinder 2 and 3 is given by:

$$p_{ii} = \left( P - \frac{\sigma_s k_2^2 - 1}{2 k_2^2} \right) \dots \dots \dots 3.31$$

When we shrink-fit layer 1 to  $m$  into layer  $m+1$ , we can take the layer 1 to  $m$  as an inner cylinder, and take  $m+1$  layer's outer cylinder. Therefore, the radial interference pressure between layer  $m$  and layer  $m+1$  can be written as

$$\delta = r_m p_m \left( \frac{(k_{m+1}^2 + 1)}{E k_{m+1}^2 - 1} + \frac{\prod_{m=1}^n k_{m+1}^2}{E \prod_{m=1}^n k_m^2 - 1} \right) \dots \dots \dots 3.32$$

Therefore, the interference between cylinder 1 and cylinder 2 is given by:

$$\delta_i = r_2 p_i \left( \frac{(k_1^2 + 1)}{E_1 (k_1^2 - 1)} + \frac{k_2^2 + 1}{E_2 (k_2^2 - 1)} \right) \dots \dots \dots 3.33$$

The interference between cylinder 2 and cylinder 3 can be given by:

$$\delta_{ii} = r_3 p \left( \frac{(k_3^2 + 1)}{E_3 k_3^2 - 1} + \frac{k_2^2 + 1}{E_2 (k_2^2 - 1)} \right) \dots \dots \dots 3.34$$

Table 3.6. Optimum geometry for the assembly of suction tube, PTFE cup and check seat

|              | Cylinder 1 (suction tube) | Cylinder 2 ( PTFE cup)  | Cylinder 3 (check seat) |
|--------------|---------------------------|-------------------------|-------------------------|
|              | 316 stainless steel       | polytetrafluoroethylene | 316 stainless steel     |
| Inner radius | 24.2                      | 16.11                   | 10.35                   |

|                                       |      |       |       |
|---------------------------------------|------|-------|-------|
| Outer radius                          | 26.8 | 24.25 | 16.15 |
| Interference between cylinder 1 and 2 | -    | 0.08  | -     |
| Interference between cylinder 2 and 3 | 0.11 | -     | -     |

### 3.4. Evaluation of stresses by using analytical technique and ANSYS simulation software

Table 3.7. Contact pressure between cylinders in MPa

|          | Analytical | ANSYS |
|----------|------------|-------|
| $P_i$    | 4.78       | 4.48  |
| $P_{ii}$ | 2.56       | 2.49  |

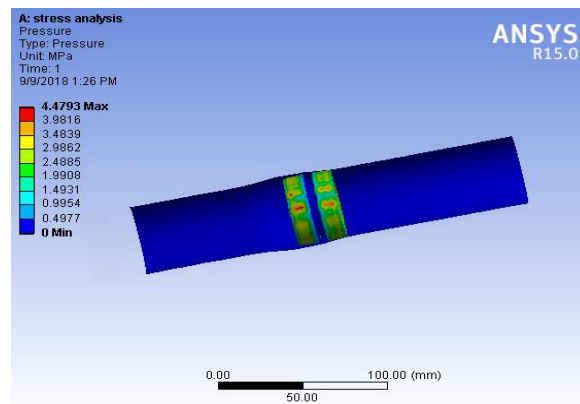


Fig 3.8. Contact pressure distribution

Table 3.8. Maximum hoop stress in MPa

| In Cylinder 1 |       | In Cylinder 2 |       | In Cylinder 3 |       |
|---------------|-------|---------------|-------|---------------|-------|
| Analytical    | ANSYS | Analytical    | ANSYS | Analytical    | ANSYS |
| 21.7          | 19.58 | 7.1           | 6.68  | 26.7          | 28.19 |

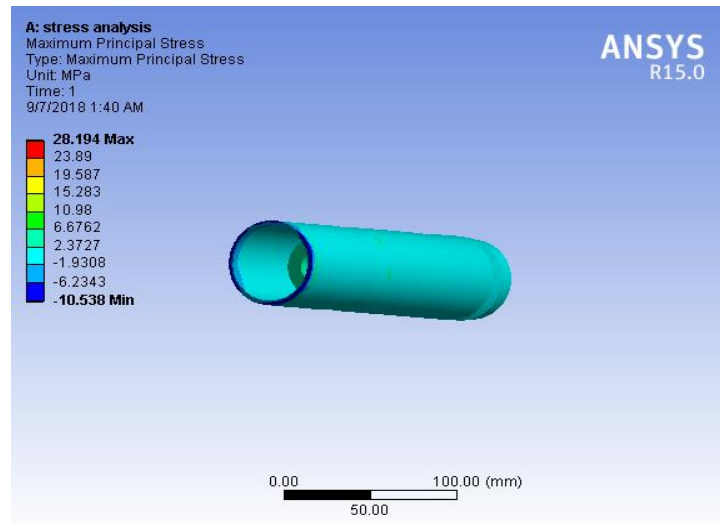


Fig 3.9. Maximum hoop stress distribution

Table 3.9. Maximum shear stress in MPa

| In Cylinder 1 |       | In Cylinder 2 |       | In Cylinder 3 |       |
|---------------|-------|---------------|-------|---------------|-------|
| Analytical    | ANSYS | Analytical    | ANSYS | Analytical    | ANSYS |
| 12.96         | 11.87 | 4.83          | 4.46  | 15.74         | 13.54 |

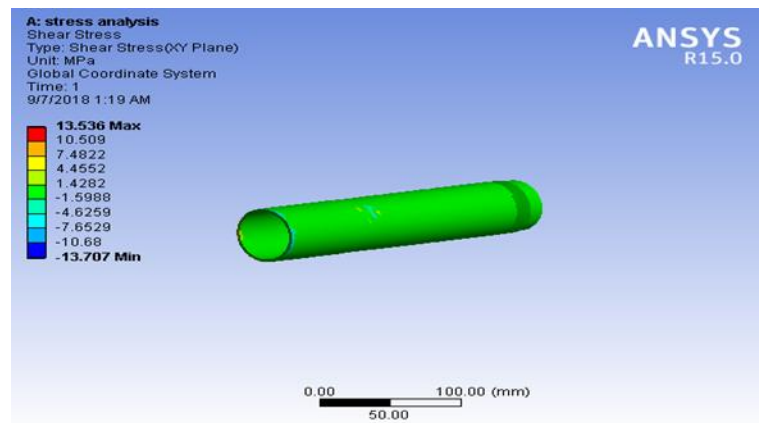


Fig 3.10. Maximum shear stress distribution

Table 3.10. Von -Mises stress in MPa

| In Cylinder 1 | In Cylinder 2 | In Cylinder 3 |
|---------------|---------------|---------------|
|---------------|---------------|---------------|



|            |       |            |       |            |       |
|------------|-------|------------|-------|------------|-------|
| Analytical | ANSYS | Analytical | ANSYS | Analytical | ANSYS |
| 24.08      | 24.99 | 8.67       | 9.37  | 29.38      | 28.12 |

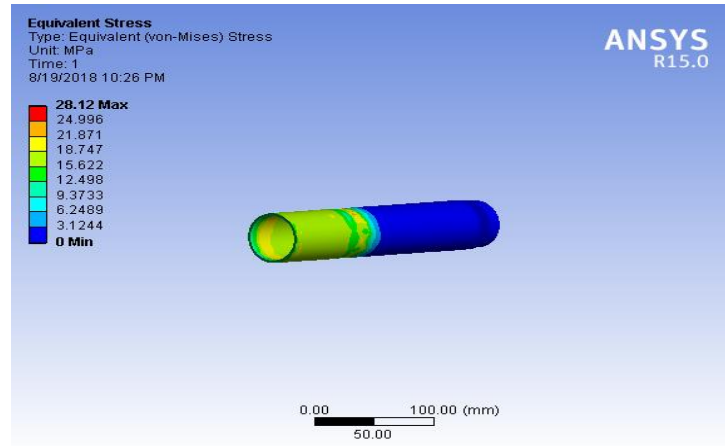


Fig 3.11. Equivalent von-Mises stress distribution

#### 4. Results and Discussions

Comparing the optimized value with that of non-optimized compound cylinder yields the following results.

Table 4.1: Comparisons of optimized contact pressure with the existing contact pressure

|            |     | Non-optimized | optimized |
|------------|-----|---------------|-----------|
| Analytical | Pi  | 7.142         | 2.56      |
|            | Pii | 9.549         | 4.78      |
| ANSYS      | Pi  | 7.934         | 4.48      |
|            | Pii | 10.007        | 2.49      |

As it can be seen from table 4.1. The contact pressure has been reduced. This implies that when the contact pressure between two contacting surfaces is low, the vulnerability to wear will also be reduced. Figure 4.1 showed the distribution of contact pressure versus interference graphs which has both optimum and non-optimum values. As we can see from the figure the optimized value of contact pressure is lower than the non-optimized value of the contact pressure.

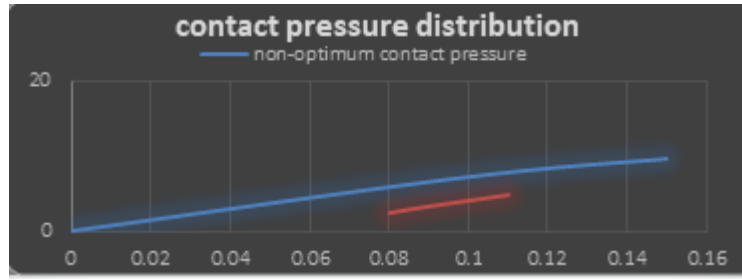


Figure 4.1: Interference versus contact pressure distribution Graph

The hoop stress or the stress along the tangential direction is optimized as shown in the following Table 4.2. From the tabulated result one can understand that the hoop stresses are distributed optimally in the three cylinders.

Table 4.2: Comparisons of optimized maximum hoop stress with the existing hoop stress

|            | In Cylinder 1 |         | In Cylinder 2 |         | In Cylinder 3 |         |
|------------|---------------|---------|---------------|---------|---------------|---------|
|            | non-optimum   | Optimum | non-optimum   | Optimum | Non-optimum   | Optimum |
| Analytical | 72.495        | 21.7    | 22.035        | 7.1     | 14..063       | 26.7    |
| Ansys      | 81.966        | 19.58   | 23.487        | 6.68    | 11.792        | 28.19   |

The tabulated results of the optimum and non-optimum values were compared in the thickness versus hoop stress graph as shown in figure 4.2. As we can see from the graph the distribution of hoop stress in the non-optimized assembly was not optimum and we can see that the stresses are not distributed optimally in the non-optimized compound cylinders. But we can see that the hoop stress distribution in the optimized compound cylinder is smoothly distributed.

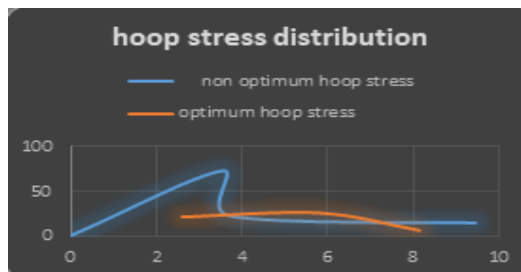


Figure 4.2: thickness versus hoop stress graph

Based on the maximum shear stress theory the following shear stress result has been found. We can see that the effect of shear stress on the compound cylinders have been improved or its effect is distributed in the three cylinders (Table 4.3).

Table 4.3: comparisons of optimized shear stress with the existing shear stress

|            | Cylinder 1  |         | Cylinder 2  |         | Cylinder 3  |         |
|------------|-------------|---------|-------------|---------|-------------|---------|
|            | Non-optimum | Optimum | Non-optimum | Optimum | non-optimum | Optimum |
| Analytical | 41.24       | 12.96   | 12.67       | 4.83    | 10.6        | 15.74   |
| Ansys      | 40.62       | 11.87   | 14.51       | 4.46    | 11.6        | 13.54   |



Figure 3.14: thickness versus shear stress graph

Comparison of shear stress versus thickness shows that there was uneven shear stress distribution in the assembly (Figure 4.3). From this graph we can see that the shear stress distribution in the non-optimized cylinder was higher and also its distribution was not smooth. The optimized compound cylinder has a good distribution of shear stresses along the thickness.

Table 4.4: comparisons of optimized von Mises stress with the existing von Mises stress

|            | In Cylinder 1 |         | In Cylinder 2 |         | In Cylinder 3 |         |
|------------|---------------|---------|---------------|---------|---------------|---------|
|            | non-optimum   | Optimum | non-optimum   | Optimum | non-optimum   | Optimum |
| Analytical | 78.163        | 24.08   | 28.056        | 8.67    | 18.631        | 29.38   |
| Ansys      | 73.188        | 24.99   | 32.528        | 9.37    | 16.27         | 28.12   |

As we can see in table 4.4, the values of the optimized and non-optimized for the cylinders are tabulated. it can be seen that the value of von-mises stress is reduced in the optimized cylinders. Figure 4.4 showed the distribution of von-mises stress versus thickness of the cylinders. as we can see from the graph the von-mises' stresses distribution in the non-optimized cylinder is not smooth as compared to the optimized ones.

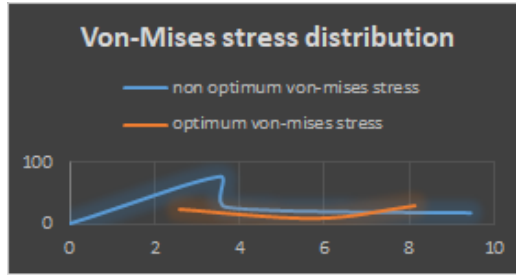


Figure 4.4: Thickness versus Von-Mises stress graph

## 5. Conclusion

During the mechanical strength analysis of the plunger pumps critical components, the bottom end of the pump was which constitutes the suction tube, PTFE cup, and check seat were assumed as a shrink-fitted tri-layer compound cylinders and the analysis were done by using the lame's theory of compound cylinders. From the analysis it can be concluded that during the assembly of the shrink-fitted compound cylinders the value of the interference between the cylinders has a great role. As we can see from the non-optimized compound cylinders the PTFE cup were damaged because of the higher contact pressure created during the sliding of the plunger. The cause of this higher contact pressure is the value of the interference given to prevent the leakage of fluid. During the optimization of the sub-assemblies of the plunger pump the value of the interference between the shrink fitted compound cylinders and the thickness were optimized and a good result was obtained as compared to the non-optimized compound cylinders.

## References

- Farrahi, M.K. Pipelzadeh, A. Akbari (2010): Residual stress analysis of autofrettaged thick-walled spherical pressure vessel. published on 26 April 2010 International Journal of Pressure Vessels and Piping 87 (2010)
- G.H. Majzoobi, G.H. Farrahi, M.K. Pipelzadeh, A. Akbari (2004): Experimental and finite element prediction of bursting pressure in compound cylinders. published on 14 June 2004 International Journal of Pressure Vessels and Piping (Elsevier publishers)
- Hamid Jahed (2005): Optimum Autofrettage and Shrink-Fit Combination in Multi-Layer Cylinders. Published on 8, 2005 Journal of Pressure Vessel Technology (ASME)
- Hong fang Lu and Shijuan Wu (2016): Vibration and Stress Analyses of Positive Displacement Pump Pipeline Systems in Oil Transportation Stations. Published on July 14, 2016, journal of pipe line system engineering (ASCE) 2016, 7(1).

- Kaoutar Bahoum, Mohammed Diany and Mustapha Mabrouki (2016): Stress analysis of compound cylinders subjected to thermo-mechanical loads. published on November 30, 2016, Journal of Mechanical Science and Technology
- Kaufmann A. (2018): Modeling dry wear of piston rod sealing elements of reciprocating compressors considering gas pressure drop across the dynamic sealing surface. Published on 03 January/ 2018 Journal of Tribology American society of mechanical engineers.
- Khurmi, R.S. J.K. Gupta (2005): text book of machine design.
- Mojtaba Sharifi, M. R. Hematiyan (2012): A new analytical solution for the optimum design of shrink-fit multi-layer compound cylinders. Published in Proceedings of the ASME July 15-19, 2012 Pressure Vessels & Piping Conference, Toronto, Ontario, Canada.
- Onur Güngör (2017): An approach for optimization of the wall thickness (weight) of a thick-walled cylinder under axially non-uniform internal service pressure distribution. Published on 20 April 2017 Defense Technology. (Elsevier publishers)
- Ossama R. Abdelsalam K. (2013): Design Optimization of Compound Cylinders Subjected to Autofrettage and Shrink-Fitting Processes. Published on March 18, 2013, Journal of Pressure Vessel Technology. ASME
- Priit Põdra, Soeren Andersson (1999): Simulating sliding wear with finite element method. published on 25 March 1999, Journal of Tribology International (Elsevier Publishers) 32 (1999) 71–81
- Rahman Seifi (2018): Maximizing working pressure of auto frettaged three-layer compound cylinders with considering Bauschinger effect and reverse yielding. Published on 9 February 2018 (Springer journal)
- Richard G. Budynas, J. Keith Nisbett (2006): text book of Shigley's Mechanical Engineering Design, Eighth Edition
- Schneider and Krenzler (2017): Dimensioning of thick-walled spherical and cylindrical pressure vessels. Published on 10 May 2017 Mathematics and Mechanics of Solids (sage publishers)
- Stanisław Stupkiewicz and, Artur Marciniśzyn (2009): Elastohydrodynamic lubrication and finite configuration changes in reciprocating elastomeric seals. Published on 11 October 2008 Journal of Tribology International (Elsevier Publishers) 42 (2009) 615–627:
- Sunil A. Patil (2005): Optimum design of compound cylinders used for storing pressurized fluids. Published in 2005 ASME International Mechanical Engineering Congress and Exposition.

- Vincenzo Vullo (2014): Text book for Circular Cylinders and Pressure Vessels Stress Analysis and Design (springer publishers)
- Xin Li, Gaoliang Peng, Wenjian Liu, and Zhe Li (2015): Research on dynamic simulation method of leakage prediction for the hydraulic system. published in the Journal of Mechanical Engineering Science (SAGE Publishers), Vol. 229(4) 771–786:
- Xu Zhenyu (2015): The Research on Pulsation of Pump Pressure in Water Mist System. Published on 2015, The 12th International Conference on Combustion & Energy Utilization (Elsevier publishers) 66 (2015) 73 – 76:
- Yasser M. Shabana, A. Elsayaf, Haitham Khalaf, Younes Khalil (2017): Stresses minimization in functionally graded cylinders using particle swarm optimization technique. Published on 29 May 2017 International Journal of Pressure Vessels and Piping. (Elsevier publishers)
- Ye Zibo, Huang Xing, Liang Rongguang (2010): Sealing Performance and Wear Mechanism of PTFE Oil Seal. Published on January 2010, advanced tribology (Springer publishers) page 287-291
- Zhou Y., Zhiqiang Huang, Yan Bu, Chengsong Qiu, Yuan Yuan (2014): Drilling mud pump plunger seals failure under ultra-high and ultra-deep conditions. Published on 15 July Engineering Failure Analysis (Elsevier publisher) 45 (2014) 142–150
- Yuan Gexia (2010): Optimum Design for Shrink-fit Multi-Layer Vessels under Ultrahigh Pressure Using Different Materials. By: et al. Published on October 20, 2010 Chinese journal of mechanical engineering (springer publishers).